Title

Bioactive potential of silica coatings and its effect on the adhesion of proteins to titanium implants

Authors

F. Romero-Gavilan[1*], N. Araújo-Gomes[1,2*&], A.M. Sánchez-Pérez[2], I. García-Arnáez[2], F. Elortza[4], M Azkargorta[4], J.J. Martín de Llano[5], C. Carda[5], M. Gurruchaga[3], J. Suay[1], I. Goñi[3]

[1] Departamento de Ingeniería de Sistemas Industriales y Diseño. Universitat Jaume I, Av. Vicent-Sos Baynat s/n. Castellón 12071. Spain.

[2] Department of Medicine. Universitat Jaume I, Av. Vicent-Sos Baynat s/n. Castellón 12071. Spain.

[3] Facultad de Ciencias Químicas. Universidad del País Vasco. P. M. de Lardizábal, 3. San Sebastián 20018. Spain.

[4] Proteomics Platform, CIC bioGUNE, CIBERehd, ProteoRed-ISCIII, Bizkaia Science and Technology Park, 48160 Derio, Spain.

[5] Department of Pathology and Health Research Institute of the Hospital Clínico (INCLIVA), Faculty of Medicine and Dentistry, University of Valencia, 46010 Valencia, Spain

[*]Co-authorship.

[&]Corresponding author: Nuno Araújo-Gomes

e-mail: araujoda@uji.es

telephone number: +34964728773

Abstract

There is an ever-increasing need to develop dental implants with ideal characteristics to achieve specific and desired biological response in the scope of improve the healing process post-implantation. Following that premise, enhancing and optimizing titanium implants through superficial treatments, like silica sol-gel hybrid coatings, are regarded as a route of future research in this area. These coatings change the physicochemical properties of the implant, ultimately affecting its biological characteristics. Sandblasted acid-etched titanium (SAE-Ti) and a silica hybrid sol-gel coating (35M35G30T) applied onto the Ti substrate were examined. The results of *in vitro* and *in vivo* tests and the analysis of the protein layer adsorbed to each surface were compared and discussed.

In vitro analysis with MC3T3-E1 osteoblastic cells, showed that the sol-gel coating raised the osteogenic activity potential of the implants (the expression of osteogenic markers, the alkaline phosphatase (ALP) and IL-6 mRNAs, increased). In the *in vivo* experiments using as model rabbit tibiae, both types of surfaces promoted osseointegration. However, the coated implants demonstrated a clear increase in the inflammatory activity in comparison with SAE-Ti. Mass spectrometry (LC-MS/MS) analysis showed differences in the composition of protein layers formed on the two tested surfaces. Large quantities of apolipoproteins were found attached predominantly to SAE-Ti. The 35M35G30T coating adsorbed a significant quantity of complement proteins, which might be related to the material intrinsic bioactivity, following an associated, natural and controlled immune response.

The correlation between the proteomic data and the *in vitro* and *in vivo* outcomes is discussed on this experimental work.

Keywords:

Dental implants, apolipoproteins, osteoimmunology, osteogenesis, bone regeneration, proteomics

1. Introduction

Titanium is a material often used in dental implants due to its high biocompatibility, resistance to corrosion and good mechanical properties, such as its strength and relatively low modulus of elasticity [1]. These are excellent characteristics for biomedical purposes. However, specific surface treatments might enhance the bioactivity of titanium devices, leading to the desired biological response [2]. Such surface modifications are designed to boost osseointegration in dental implants, improving tissue healing [3].

The degree of integration of a biomaterial in a living organism depends on the interaction of many factors in the microenvironment formed after the implantation. The first layer of proteins adsorbed onto the biomaterial surface might have a strong effect on the development and activation of several biological processes. The success of implantation might depend on these proteins, spreading and adsorbing on the surface by competitive displacement (Vroman effect) [4].

Coagulation cascades, complement system pathways, platelets and immune cells are activated and become involved immediately in the microenvironment formed after the surgical procedure, starting the process of inflammation [5]. The deposition of the proteins activating these processes depends on distinct features of the surfaces. The preferential adsorption of certain types of proteins might be associated with the specific physical and chemical properties of these materials [6]. Hence, controlling the amount, type and the conformation of the adhering proteins is of the utmost importance in promoting the correct, fast tissue regeneration. It is vital to obtain a moderate and natural immune response (not a chronic inflammation) to the biomaterial. Such a response should favour the regeneration and good osseointegration, thus contributing to the success of the implantation [7].

The use of silica sol-gel hybrid materials in biomedical applications is becoming increasingly widespread [8–10]. The versatility of the sol-gel techniques allows tuning

the final physicochemical properties of a biomaterial by selection of appropriate precursors and optimisation of synthesis parameters [11]. The hybrid silica sol-gel materials can be applied easily as a coating onto titanium, bioactivating the surface and conferring the desired properties to the implants. These coatings are biocompatible and biodegradable, with osteoinductive properties due to the release of silicon compounds during their hydrolytic degradation [8–10]. Silicon is an essential element in bone metabolism and it is involved in the formation and mineralisation of this tissue [12].

The behaviour of sandblasted, acid-etched titanium (SAE-Ti) and a hybrid silica sol-gel coating applied onto this substrate was compared using *in vitro* and *in vivo* tests. The pattern of proteins adsorbed onto these two surface types was analysed. Then, the results of the proteomic study of protein–biomaterial interactions were compared with the outcomes of *in vitro* and *in vivo* studies.

2. Materials and methods

2.1. Titanium discs

Ti discs (12 mm in diameter, 1-mm thick) were made from a bar of commercially available, pure, grade-4 Ti (Ilerimplant-GMI S.L., Lleida, Spain). To obtain the sandblasted, acid-etched (SAE) Ti, the discs were abraded with 4-μm aluminium oxide particles and acid-etched by submersion in sulfuric acid for 1 h, to simulate a moderately rough implant surface. Discs were then washed with acetone, ethanol and 18.2-Ω purified water (for 20 min in each liquid) in an ultrasonic bath and dried under vacuum. Finally, all Ti discs were sterilised using UV radiation.

2.2. Sol-gel synthesis and sample preparation

The silica hybrid material was obtained through the sol-gel route. The precursors used were the alkoxysilanes: methyltrimethoxysilane, 3-(glycidoxypropyl)-trimethoxysilane and tetraethyl orthosilicate (Sigma-Aldrich, St. Louis, MO, USA) in molar percentages of 35%, 35% and 30%, respectively. This composition, 35M35G30T, was chosen based on previous studies [8]. 2-Propanol (Sigma-Aldrich, St. Louis, MO, USA) was used as a solvent in the synthesis at a volume ratio (alcohol:siloxane) of 1:1. Hydrolysis of alkoxysilanes was carried out by adding (at a rate of 1 drop s^{-1}) the corresponding stoichiometric amount of acidified aqueous solution of 0.1M HNO_3 (Panreac, Barcelona, Spain). The mixture was kept for 1 h under stirring and then 1 h at rest. The samples were prepared immediately afterwards. SAE-titanium was used as the substrate for the sol-gel coating. The coating was performed employing a dip-coater (KSV DC; KSV NIMA, Espoo, Finland). Discs and implants were immersed in the sol-gel solution at a speed of 60 cm min^{-1}, left immersed for one minute, and removed at a 100 cm min^{-1}. Finally, the samples were cured for 2 h at 80 ºC.

2.3. *Physicochemical characterisation of coated titanium discs*

The surface topography of samples was characterised using scanning electron microscopy (SEM) employing the Leica-Zeiss LEO equipment under vacuum (Leica, Wetzlar, Germany). Platinum sputtering was applied to make the materials more conductive for the SEM observations. An optical profilometer (interferometric and confocal) PLm2300 (Sensofar, Barcelona, Spain) was used to determine the roughness. Three discs of each type were tested. Three measurements were performed for each disc to obtain the arithmetic average values of roughness (Ra). An atomic force microscope (AFM, Bruker Multimode, Billerica, MA, USA) was employed to evaluate the nanocomponents of roughness. Measurements were carried out at scan size of 1 μm and at scan rate of 0.3 Hz (n = 3). The results were analysed using the NanoScope Analysis software (http://nanoscaleworld.bruker-axs.com/nanoscaleworld/media/p/775.aspx). The contact angle was measured using an automatic contact angle meter OCA 20 (Dataphysics Instruments, Filderstadt, Germany). Ten μL of ultrapure water were deposited on the disc surfaces at a dosing rate of 27.5 μL s^{-1} at room temperature. Contact angles were determined using SCA 20 software (Dataphysics Instruments, Filderstadt, Germany). Six discs of each material were studied, after depositing two drops on each disc.

2.4. In vitro assays

2.4.1. Cell culture

MC3T3-E1 (mouse calvaria osteosarcoma cell line) cells were cultured on the 35M35G30T-coated and uncoated titanium discs at a concentration of 1×10^4 cells/well, in 24-well culture NUNC plates (Thermo Fisher Scientific, Waltham, MA, USA). The medium contained Dulbecco Modified Eagle Medium (DMEM) with phenol red (Gibco-Life Technologies, Grand Island, NY, USA), 1% 100× penicillin/streptomycin (Biowest Inc., Riverside, KS, USA) and 10% fetal bovine serum (FBS) (Gibco-Life Technologies,

Grand Island, NY, USA). After incubation for 24 hours at 37 ºC in a humidified (95%) atmosphere of 5% CO_2, the medium was replaced with an osteogenic medium composed of DMEM with phenol red 1×, 1% penicillin/streptomycin, 10% FBS, 1% ascorbic acid (5 mg mL^{-1}) and 0.21% β-glycerol phosphate, and incubated again under the same conditions. The culture medium was changed every 48 hours. In each plate, a well with cells at the same concentration (1×10^4 cells) was used as a control of culture conditions. In parallel, cells were allowed to differentiate for 7, 14 and 21 days before being harvested for RNA isolation.

2.4.2. Cytotoxicity

The biomaterial cytotoxicity was assessed following the ISO 10993-5 specifications, measured by spectrophotometry, after contact of the material extract with the cell line. The 96-Cell Titter Proliferation Assay (Promega®, Madison, WI, USA) was employed to measure the cell viability after 24-h incubation of the cells with the extract. One negative control (empty well) and a positive control with latex, known to be toxic to the cells were used. Seventy-percent cell viability was the limit below which a biomaterial was considered cytotoxic.

2.4.3. Cell Proliferation

For measuring cell proliferation, the commercial cell-viability assay AlamarBlue® (Invitrogen-Thermo Fisher Scientific, Waltham, MA, USA) was used. This kit measures the cell viability on the basis of a redox reaction with resazurin. The cells were cultured in wells with the discs (3 replicates per treatment) and examined following the manufacturer's protocol after 1, 3, 5 and 7 days of culture. The percentage of reduced resazurin was used to evaluate cell proliferation.

2.4.4. ALP activity

The conversion of p-nitrophenylphosphate (p-NPP) to p-nitrophenol was used to assess the ALP activity. The culture medium was removed from the wells, the wells were washed

3 times with 1 × Dulbecco's Phosphate Buffered Saline (DPBS), and 100 µL of lysis buffer (0. 2% Triton X-100, 10 mM Tris-HCl pH 7.2) was added to each. The sample aliquots of 0.1 mL were used to carry out the assay. One hundred µL of p-NPP (1 mg mL^{-1}) in substrate buffer (50 mM glycine, 1mM $MgCl_2$, pH 10.5) was added to 100 µL of the supernatant obtained from the lysate. After two hours of incubation in the dark (37 ºC, 5% CO_2), absorbance was measured using a microplate reader at a wavelength of 405 nm. ALP activity was obtained from a standard curve obtained using different solutions of p-nitrophenol and 0.02 mM sodium hydroxide. Results were presented as mmol of p-nitrophenol/hour (mmol PNP h^{-1}). The data were expressed as ALP activity normalised by the total protein content (µg $µL^{-1}$) obtained using Pierce BCA assay kit (Thermo Fisher Scientific, Waltham, MA, USA) after 7 and 14 days.

2.4.5. RNA isolation and cDNA synthesis

Total RNA was prepared from the cells grown on the sol-gel coated titanium discs, using Qiagen RNeasy Mini kit (Qiagen, Hilden, Germany), following digestion with DNaseI (Qiagen), according to the manufacturer's instructions. The quantity, integrity and quality of the resulting RNA were measured using NanoVue® Plus Spectrophotometer (GE Healthcare Life Sciences, Litlle Chafont, United Kingdom). For each sample, about 1 µg of total RNA was converted to cDNA using PrimeScript RT Reagent Kit (Perfect Real Time) (TAKARA Bio Inc., Shiga, Japan). The resulting cDNA was diluted in DNase-free water to a concentration suitable for reliable RT-PCR analysis.

2.4.6. Quantitative Real-time PCR

Prior to the RT-qPCR reaction, primers for ALP and IL6 genes were designed from specific DNA sequences for these genes available from NCBI (https://www.ncbi.nlm.nih.gov/nuccore) using PRIMER3plus software tool (http://www.bioinformatics.nl/cgi-bin/primer3plus/primer3plus.cgi). Expression levels were measured using primers purchased from Life Technologies S.A. (Gaithersburg,

MD), GADPH sense TGCCCCCATGTTTGTGATG; GADPH antisense TGGTGGTGCAGGATGCATT; ALP sense CCAGCAGGTTTCTCTCTTGG; ALP antisense CTGGGAGTCTCATCCTGAGC; IL6 sense AGTTGCCTTCTTGGGACTGA and IL6 antisense TCCACGATTTCCCAGAGAAC. All primers are listed from 5′ to 3′ and GADPH was used as a housekeeping gene to normalise the data obtained from the RT-qPCR and calculate the relative fold-change between conditions. qPCR reactions were carried out using SYBR PREMIX Ex Taq (Tli RNase H Plus) (TAKARA Bio Inc., Shiga, Japan), in an Applied Biosystems StepOne Plus™ Real-Time PCR System (Foster City, California, USA). The cycling parameters were as follows: an initial denaturation step at 95 ºC for 30 s followed by 95 ºC for 5 s and 60 ºC for 34 s for 40 cycles. The final melt curve stage comprised a cycle at 95 ºC for 15 s and at 60 ºC, for 60 s.

2.4.7. Statistical analysis

Data were submitted to one-way analysis of variance (ANOVA) and to a Newman-Keuls multiple comparison post-test, when appropriate. Differences with $p \leq 0.05$ were considered statistically significant.

2.5. *In vivo experimentation*

To assess the *in vivo* behaviour of the two biomaterials, the bare and coated dental implants were surgically placed in the tibia of New Zealand rabbits (*Oryctolagus cunicu*lus). This implantation model is widely used to study the osseointegration of dental implants [13]. All the experiments were conducted in accordance with the protocols of Ethical Committee of the Valencia Polytechnic University (Spain), the European guidelines and legal conditions laid in R. D. 223/1988 of March 14th, and the Order of October 13rd, 1988, of the Spanish Government on the protection of animals used for experimentation and other scientific purposes. The rabbits were kept under 12-h span darkness-light cycle; room temperature was set at 20.5 ± 0.5 ºC, and the relative humidity

ranged between 45 and 65%. The animals were individually caged and fed a standard diet and filtered water *ad libitum*. Dental implants were supplied by Ilerimplant S.L. (Lleida, Spain). These were internal-connection dental implants, made with titanium grade 4 (trademark GMI), of 3.75-mm diameter and 8-mm length, Frontier model with SAE surface treatment. Overall, 10 implants were used, 5 uncoated (SAE-Ti) and 5 coated with the 35M35G30T sol-gel composition. They were all implanted under the same conditions.

5 rabbits were employed to carry out the assay, all of them weighing between 2000 and 3000 g, aging near the physeal closure (indicative of an adequate bone volume). The implantation period for the experimental model was 2 weeks. Implants were inserted in both left and right proximal tibiae, each animal receiving two implants (one SAE-Ti sample and one sol-gel coated sample). Animals were sedated (chlorpromazine hydrochloride) and prepared for surgery, and then anaesthetized (ketamine hydrochloride). A coetaneous incision was made to the implantation site in the proximal tibia. The periosteum was removed, and the osteotomy was performed using a low revolution micromotor and drills of successive diameters of 2, 2.8 and 3.2 mm, with continuous irrigation. Implants were placed by press-fit, and surgical wound was sutured by tissue planes, washed with saline water and covered with plastic spray dressing (Nobecutan, Inibsa Laboratories, Barcelona, Spain). After the implantation period, animals were euthanised by carbon monoxide inhalation, and the implant screws were retrieved to study the surrounding tissues. The samples were embedded in methyl methacrylate, and 25–30 μm sections were obtained using EXAKT Technique (EXAKT Technologies, Inc., Oklahoma, USA). Slides were sequentially stained with Stevenel's blue and van Gieson's picro-fuchsin following the procedure described by Maniatopoulos *et al.* [14]. Digital images of the tissues surrounding the implant threads were recorded with a brightfield Leica DM4000 B microscope and a DFC420 digital camera using 1.6, 5, 10, 20 and 100× objectives. The bone–implant contact in the cortical region of the

implant and the length of osteoclast-like and foreign body giant cells in contact with the implant surface of threads in the medullar bone cavity were evaluated using the image-processing program ImageJ 1.48 (National Institutes of Health, USA, http://imagej.nih.gov/ij).

2.6. Adsorbed protein layer

Sol-gel-coated and uncoated titanium discs were incubated in a 24-well plate for 180 min in a humidified atmosphere (37 ºC, 5% CO_2), after the addition of 1 mL of human blood serum from male AB plasma (Sigma-Aldrich, St. Louis, MO, USA).

The serum was removed, and, to eliminate the non-adsorbed proteins, the discs were rinsed five times with ddH_2O and once with 100 mM NaCl, 50 mM Tris-HCl, pH 7.0. The adsorbed protein layer was collected by washing the discs in 0.5 M triethylammonium bicarbonate buffer (TEAB) with 4% of sodium dodecyl sulphate and 100 mM of dithiothreitol (DTT). Four independent experiments were carried out for each type of surface; in each experiment, four discs for each material were processed. The protein content was quantified before the experiment (Pierce BCA assay kit; Thermo Fisher Scientific, Waltham, MA, USA), obtaining a value of 51 mg mL^{-1}.

2.7. Proteomic analysis

Proteomic analysis was performed as described by Romero-Gavilán *et al.* [6], with minor variations. Briefly, the eluted protein was in solution digested following the FASP protocol established by Wisnewski *et al.* [15] loaded onto a nanoACQUITYUPLC system connected online to an SYNAPT G2-Si MS System (Waters, Milford, MA, USA). Each material was analysed in quadruplicate. Differential protein analysis was carried out using Progenesis software (Nonlinear Dynamics, Newcastle, UK) as described before [6], and the functional annotation of the proteins was performed using PANTHER (www.pantherdb.org/) and DAVID Go annotation programmes (https://david.ncifcrf.gov/).

3. Results

3.1. Synthesis and physicochemical characterisation

The sol-gel synthesis was carried out, and a well-adhering and homogenous coating was obtained on SAE-Ti discs. SEM micrographs showed substantial morphological differences between the bare and coated titanium discs (Figure 1a – 1d). The sol-gel material partly covered the initial roughness (shown by the data obtained using optical profilometer). After the 35M35G30T sol-gel treatment, Ra decreased to 0.79 ± 0.09 µm from its original value of 1.15 ± 0.10 µm for SAE-Ti surfaces. AFM images display the morphological properties of both surfaces on a lower scale (Figure 1e and 1f). The uncoated surface showed a Ra value of 19.00 ± 2.05 nm, while the sol-gel coating involved a reduction of the roughness nanocomponents displaying a Ra value of 1.75 ± 0.94 nm. The contact angle measurements revealed a significant increase in wettability as a consequence of coating. Uncoated and coated discs presented angles of 79.55 ± 7.51º and 50.39 ± 3.78º, respectively. Thus, the sol-gel-coated material was more hydrophilic than the initial SAE-Ti, possibly due to its hydroxyl group content [8].

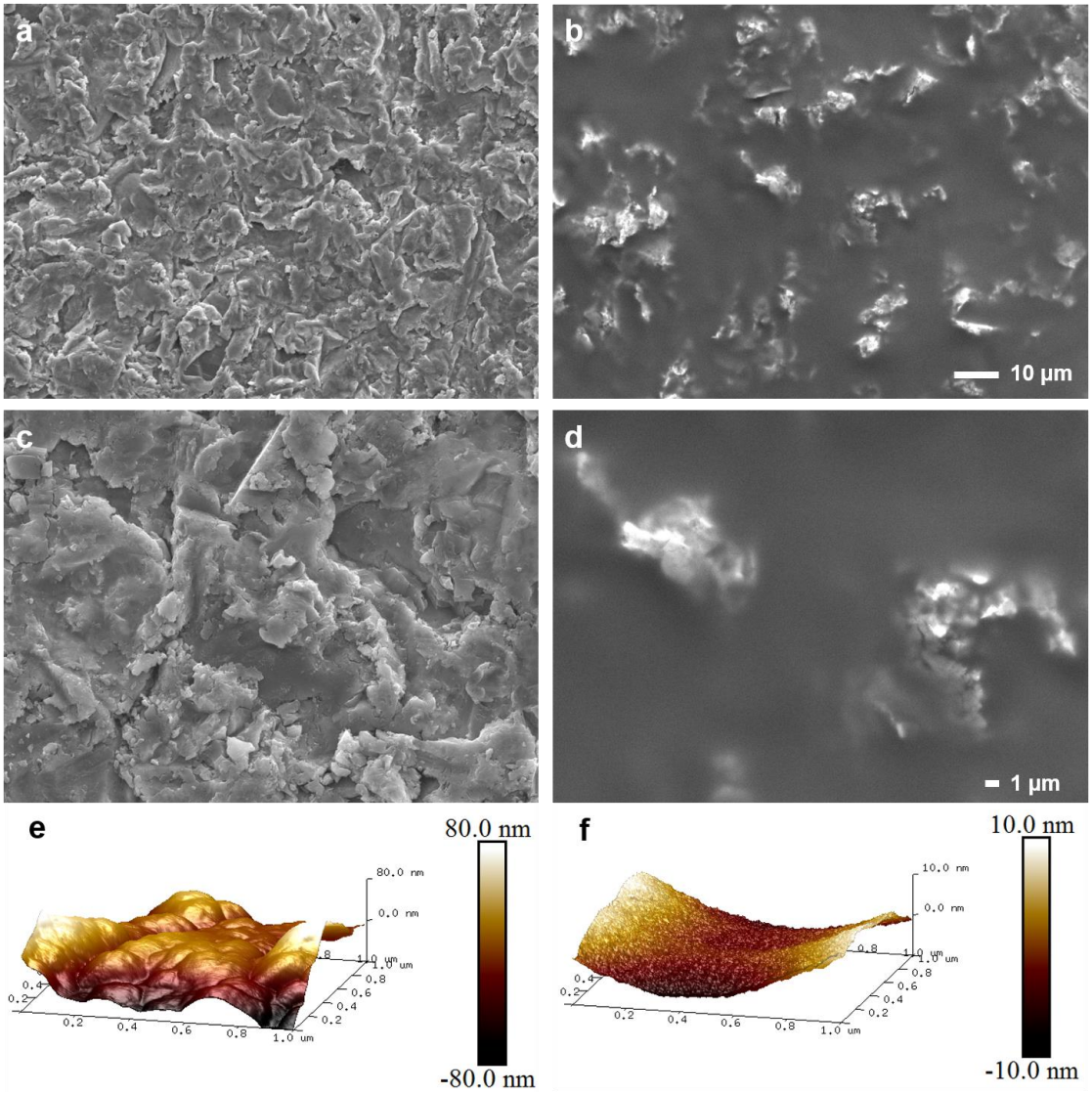

Figure 1. SEM micrographs of SAE-Ti (A and C) and hybrid sol-gel coating (B and D). Scale bars: A and B, 10 µm and C and D, 1 µm.

3.2. In vitro assays

3.2.1. Cell cytotoxicity, proliferation and ALP activity

Neither of the examined materials was cytotoxic (data not shown). The proliferation and ALP activity assays do not show significant differences between the two materials at most of the time points, except for the proliferation assay at 3 days period, in which the 35M35G30T boosts higher values of proliferation (Figure 2).

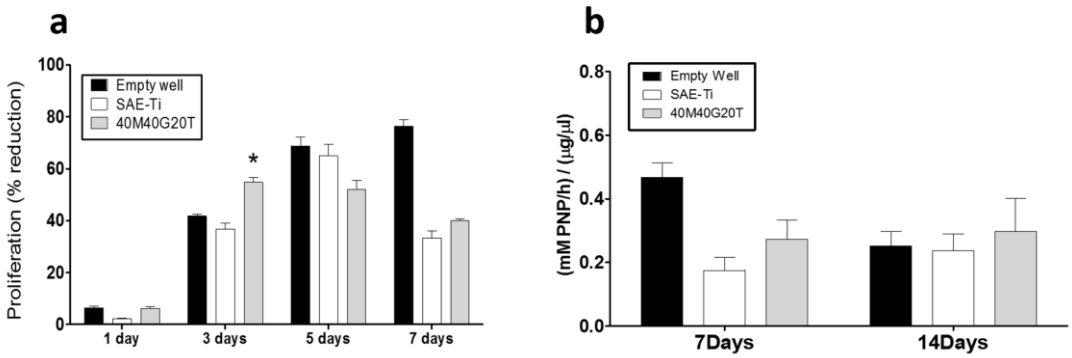

Figure 2. MC3T3-E1 *in vitro* assays: a) MC3T3-E1 cell proliferation after 1, 3, 5 and 7 days of cell culture with SAE-Ti (white bar) and 35M35G30T (grey bar). b) ALP activity (mM PNP h^{-1}), normalised to the amount of total protein (µg μL^{-1}), in the MC3T3-E1 cells cultivated on SAE-Ti (white bar) and 35M35G30T formulation (grey bar). Cells in an empty well were used as a positive control (black bar). Statistical analysis was performed using one-way ANOVA with a Kruskal-Wallis post- test (*, $p \leq 0.05$).

3.2.2. mRNA expression levels

After 14 days of incubation, there were found large and statistically significant differences ($p < 0.001$) between mRNA expression levels for ALP and IL-6 in the cells cultivated on 35M35G30T discs and those grown on SAE-Ti and the blank controls (Figure 3), showing the bioactive potential of this coating formulation.

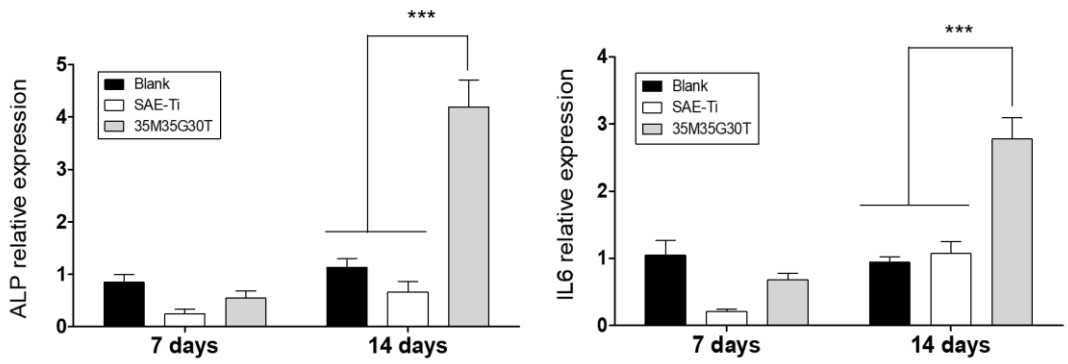

Figure 3. Gene expression of osteogenic markers (a) ALP and (b) IL6 on MC3T3-E1 osteoblastic cells cultured on SAE-Ti (white bar) and 35M35G30T (grey bar). Cells in an empty well were used as a positive control (black bar). The relative mRNA expression was determined by RT-PCR after 7 and 14 days of cell culture. Statistical analysis was performed using one-way ANOVA with a Kruskal-Wallis post-test (***, $p \leq 0.001$).

3.3. In vivo experimentation

No statistically significant differences were found between osseointegration levels for the uncoated (SAE-Ti) and sol-gel-coated implants during the studied period (Figure 4, A-B). On the coated implants, transparent layers of undegraded material (Figure 4, B and D) were observed in the deep areas of the screw grooves. This coating layer was thinner or absent in the threads in contact with or next to the bone tissue. It was more evident in the grooves of the implant located in the medullary cavity of the bone and away from the trabeculae of bone tissue. Along this medullary zone, in the implant–tissue interface (SAE-Ti samples) or coating–tissue interface (35M35G30T samples), were observed connective tissue, inflammatory components and two types of multinucleated cells. One of these cell types had the size and morphological characteristics similar to osteoclasts, and the other was composed of larger cells, similar to foreign body giant cells (Figure 4, C-D and insets). The length of that interface and the length of the osteoclast-like and giant cells were measured. The cells shorter than 100 µm were considered osteoclast-

like cells and the larger cells were classified as giant cells. Osteoclastic cells from the uncoated and coated implants were of similar length (44.4 ± 21.6 µm, N = 272 and 40.4 ± 27.9 µm, N = 50, respectively). The giant cells were smaller in the SAE-Ti than in 35M35G30T samples (cell length 162.0 ± 73.6 µm, N = 66 and 268.0 ± 140.0 µm, N = 46, respectively). The difference was statistically significant ($p < 0.001$, non-parametric Mann–Whitney test). In the coated implants, the areas of bone regeneration showed fewer giant cells, and fibrous capsules between the bone tissue and implant were not observed.

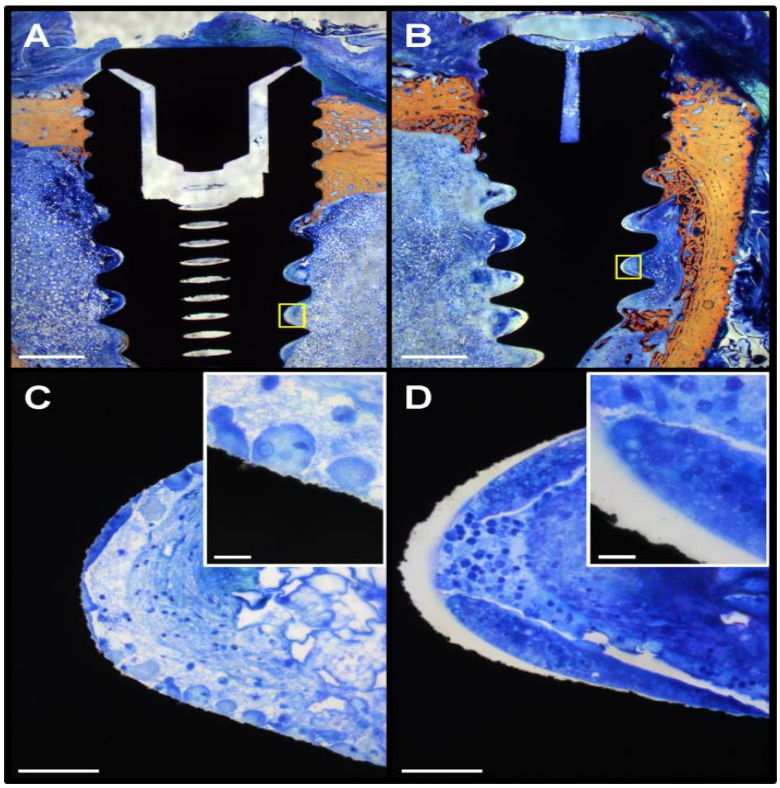

Figure 4. Microphotographs of SAE-Ti and 35M35G30T samples. Panoramic images of SAE-Ti (A) and 35M35G30T (B) samples show the implant regions close to the cortical bone and in the medullary cavity. The regions enclosed in white-edged squares in A and B are shown in panels C and D, respectively. In the panel C, several rounded and elongated osteoclast-like and giant cells touch the surface of the implant. In the D panel, two giant cells, flanking a region with inflammatory cells, are in contact with the transparent coating of the implant surface. Lower regions of the C and D images are

shown magnified in the corresponding insets. Stevenel's blue and van Gieson's picro-fuchsin staining was used. Scale bars: A and B, 1 mm; C and D, 0.1 mm; insets, 0.02

3.4. Proteomic analysis

LC-MS/MS analysis detected and identified 133 proteins for each material. Progenesis QI software was employed to study differences between protein adsorption on the SAE-Ti and hybrid silica-treated surfaces. DAVID and PANTHER tools were used to classify these proteins according to their function.

The comparison of the characteristic proteins attached to the two biomaterials showed that 16 proteins were more abundant on the SAE-Ti than on the coated surfaces (Table 1).

Table 1. Progenesis analysis of proteins differentially attached to SAE-Ti.

Description	Accession	Confidence score	Average SAE-Ti	Average 35M35G30T	ANOVA (p)	Ratio SAE-Ti/ 35M35G30T
Platelet factor 4 variant	PF4V_HUMAN	106.83	2.05E+05	3.95E+03	6.62E-04	52.00
Coagulation factor XI	FA11_HUMAN	337.82	2.21E+05	9.18E+03	4.67E-02	24.06
Apolipoprotein C-IV	APOC4_HUMAN	80.60	1.18E+05	5.39E+03	3.91E-05	21.81
Vitamin K-dependent protein C	PROC_HUMAN	124.64	2.08E+05	1.36E+04	4.21E-03	15.27
Serum amyloid A-4 protein	SAA4_HUMAN	150.29	2.24E+06	2.11E+05	1.09E-04	10.60
Creatine kinase M-type	KCRM_HUMAN	104.21	1.58E+04	1.74E+03	1.66E-03	9.06
Prothrombin	THRB_HUMAN	375.17	1.91E+06	2.72E+05	1.15E-03	7.02
Apolipoprotein E	APOE_HUMAN	1836.86	2.54E+07	4.62E+06	9.73E-03	5.51
Vitronectin	VTNC_HUMAN	430.96	1.03E+07	2.06E+06	3.53E-04	4.98
Apolipoprotein C-I	APOC1_HUMAN	163.40	3.22E+06	6.53E+05	9.19E-03	4.94
Apolipoprotein A-V	APOA5_HUMAN	134.27	4.82E+04	1.03E+04	2.61E-04	4.67
Selenoprotein P	SEPP1_HUMAN	242.92	1.99E+05	6.33E+04	4.35E-03	3.14
Apolipoprotein(a)	APOA_HUMAN	108.16	8.15E+04	3.90E+04	3.74E-02	2.09
Apolipoprotein A-IV	APOA4_HUMAN	1044.44	1.36E+06	7.07E+05	2.24E-02	1.92
Apolipoprotein A-I	APOA1_HUMAN	1051.15	1.25E+07	6.68E+06	1.19E-03	1.87
Apolipoprotein C-II	APOC2_HUMAN	133.73	3.20E+05	1.85E+05	4.09E-02	1.73

The list in Table 1 shows some proteins related to blood coagulation processes, such as FA11, THRB and PROC. Notably, a large number of apolipoproteins adsorbed preferentially to the titanium surface in comparison with the sol-gel material (APOA, APOA1, APOA4, APOA5, APOC1, APOC2, APOC4 and APOE), as well as SAA4, classified as high-density lipoprotein by DAVID. PF4V, KCRM, VTNC and SEPP1 were also identified as more abundant in SAE-Ti elutions.

PANTHER chart in Figure 5a displays the classification of biological processes in which the proteins characteristic for titanium surfaces are involved. Among the identified processes, the most significant were the cellular (14%) and metabolic (16%) processes and the response to stimulus (16%). Molecules with functions related to the immune system were also detected although they constituted only 2% of the proteins.

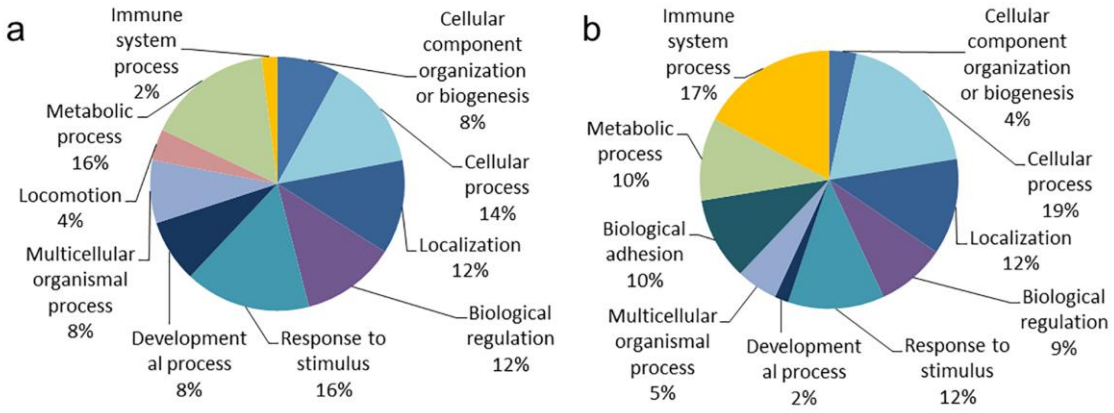

Figure 5. PANTHER pie chart of the biological processes associated with the proteins differentially adhering to SAE-Ti (a) and 35M35G30T (b).

Table 2 shows the 20 proteins more predominant on the 35M35G30T biomaterial than on untreated surfaces. A large proportion of these proteins is related to the immune response and the complement system, such as C1R, CO5, CO6, CO7, CO8A and CO8B proteins and the immunoglobulins IGJ, IGHA1 and IGHM. The proteins AFAM, HPT, A1AT and A2MG were also detected.

Table 2. Progenesis analysis of proteins differentially attached to silica sol-gel coating.

Description	Accession	Confidence score	Average SAE-Ti	Average 35M35G30T	ANOVA (p)	Ratio 35M35G30T /SAE-Ti
Complement component C6	CO6_HUMAN	100.06	1.02E+04	3.02E+04	5.20E-03	2.97
Complement factor H-related protein 2	FHR2_HUMAN	253.29	3.93E+04	1.07E+05	4.31E-03	2.72
Immunoglobulin J chain	IGJ_HUMAN	123.70	1.30E+05	3.41E+05	1.29E-02	2.62
Ceruloplasmin	CERU_HUMAN	338.22	5.49E+04	1.36E+05	8.43E-03	2.48
Alpha-1-antitrypsin	A1AT_HUMAN	466.15	4.73E+05	1.15E+06	6.21E-04	2.44
Alpha-1-acid glycoprotein 1	A1AG1_HUMAN	171.81	4.74E+04	1.14E+05	1.41E-02	2.41
Complement component C7	CO7_HUMAN	358.70	7.98E+04	1.85E+05	1.78E-02	2.32
Ig mu chain C region	IGHM_HUMAN	262.24	1.92E+05	4.32E+05	2.25E-02	2.25
Alpha-1-antichymotrypsin	AACT_HUMAN	490.40	7.31E+04	1.63E+05	4.01E-03	2.23
Serotransferrin	TRFE_HUMAN	1935.92	2.56E+06	5.58E+06	1.26E-02	2.18
Complement C5	CO5_HUMAN	620.04	4.90E+04	1.07E+05	2.10E-02	2.18
Haptoglobin	HPT_HUMAN	755.00	5.13E+05	1.09E+06	7.85E-03	2.13
Serum albumin	ALBU_HUMAN	2067.21	2.34E+07	4.96E+07	1.70E-02	2.12
Complement component C8 alpha chain	CO8A_HUMAN	193.83	8.99E+04	1.88E+05	1.43E-02	2.09
Complement component C8 beta chain	CO8B_HUMAN	96.20	1.45E+04	3.01E+04	8.01E-03	2.08
Ig alpha-1 chain C region	IGHA1_HUMAN	386.53	7.00E+05	1.44E+06	7.20E-03	2.06
Complement C1r subcomponent	C1R_HUMAN	306.85	1.33E+05	2.52E+05	4.79E-03	1.90
Retinol-binding protein 4	RET4_HUMAN	79.55	7.64E+04	1.42E+05	3.37E-02	1.85
Alpha-2-macroglobulin	A2MG_HUMAN	669.00	1.91E+05	3.45E+05	1.81E-02	1.81
Afamin	AFAM_HUMAN	188.26	3.52E+04	6.32E+04	1.68E-02	1.80

For the 35M35G30T samples, PANTHER analysis identified, among others, protein functions associated with cellular (19%) and metabolic (10%) processes, in similarity to the titanium-only results. However, in this case, the proportion of proteins related to immune system processes reached 17% (Figure 5b).

4. Discussion

There is an ever-increasing interest and research on the biomaterial science industry for the development of implants with bioactive properties in the scope of decreasing the recovery times following the post-implantation procedure. Chemical and physical surface modifications of the implants are state-of-the-art areas in which researchers focus their attention, due to the fact that these modifications can ultimately influence cell behavior [16]. To a large extent, this behaviour is affected by the proteins attached to the surface of the implant, representing a microenvironment whose characteristics determine the success of the implantation [17]. It is widely known that the titanium is not, by itself, bioactive; even though it has osteoconductive properties, it is not osteoinductive [2]. To confer osteoinductive characteristics to the titanium devices, imply the modification of the physicochemical properties of their surfaces. This alters the conformation, quantity and type of proteins that attach to the implant in contact with biological fluids [18].

This experimental study was designed to compare and characterise two distinct surfaces, one an uncoated sandblasted acid-etched titanium (SAE-Ti), and the other coated with a silica sol-gel hybrid 35M35G30T biomaterial, regarding their physicochemical properties, *in vitro* and *in vivo* behaviour and the characterization of the protein layer adsorption onto each surface.

Apart from the obvious chemical differences between the titanium surfaces and silicon coatings, their morphological characterisation revealed specific properties of these

surfaces, showing that the application of the sol-gel coating decreases surface roughness at micro and nano-level and increases hydrophilicity. These distinct characteristics might ultimately affect both the protein adsorption and the biological behaviour of the biomaterial. Indeed, *in vitro* results demonstrated an increase in the bioactive potential of the sol-gel-coated implant in comparison with the uncoated titanium. In particular, it was observed changes in the mRNA expression levels, as it was found an almost 4-fold increase in the expression of the ALP mRNA and at least 2-fold increase in the expression of the mRNA for IL6 (Figure 3). ALP is expressed early in the development of the bone and during cartilage calcification [19] and is a well-known biomarker for osteoblastic differentiation. This marker has been used for the assessment of fracture healing [20]. IL-6 is a regulator of the differentiation of pre-osteoblastic cells and initiates apoptosis in the mature osteoblasts. Moreover, the expression of its receptor is high during differentiation of osteoblasts *in vitro* [21]. It has also been reported as a direct stimulator of RANKL and OPG mRNA expression in the mouse bone tissue [22], promoting prostaglandin production and, thus, modulating the inflammatory potential [23]. Interestingly, IL-6 can act as an ALP induction factor during the inflammatory phase of wound repair in the skin [24] and even in bone tissue remodelling [25]. Therefore, the 35M35G30T material might have a role in promoting osteoblastic activity.

In vivo results for the two examined surfaces did not show clear differences in bone repair during the tested period even though the *in vitro* experiments demonstrated higher bioactivity in the coated samples. Nevertheless, there was a significant increase in the immune complex activation on the sol-gel-coated implants. This was demonstrated by the higher abundance of the foreign body giant cells (FBGC) surrounding the residual areas of non-degraded material, in comparison with the SAE-Ti (Figure 4). The presence of FBGCs in degradable materials is quite common as their activity is needed for the recovery of the implanted tissue. Without it, immune structures like thick fibrous capsules

might be formed around the material, with all the associated disadvantages [26]. In fact, for the coated surfaces, in the areas of bone regeneration, it occurs a clear decrease in the number of giant cells and no presence of fibrotic tissue.

The comparison between the composition of protein layers on SAE-Ti and 35M35G30T coating revealed many proteins differentially attached to these surfaces. This distinct affinity of some proteins to these materials could be attributed to their different physicochemical properties such surface chemistry, wettability or roughness [27,28]. In this sense, for example, an increase in surface roughness could be involved with changes in the adsorption of specific proteins [29].

Interestingly, among the protein group characteristic for titanium, the PF4V protein was the most abundant (52-fold increase in comparison with the sol-gel treated samples). This protein is a platelet chemokine inhibiting both angiogenesis and tumour growth [30]. However, its specific role in bone regeneration processes remains unclear. Remarkably, a large number of apolipoproteins were attached predominantly to the SAE-Ti surface. Cho *et al.* have reported that apolipoproteins might prevent the activation of innate immunity response, and have an anti-inflammatory potential [31]. These results indicate that the high biocompatibility of titanium might be related to the preferential adsorption of this family of proteins onto its surface. Other studies suggest that the immunomodulatory role of apolipoproteins might be associated with the polarisation of macrophages in their anti-inflammatory phenotype [32,33]. Similarly, VTNC has been identified as an inhibitor of the complement cascade activation [34]. This protein has an important role in the interleukin IL-4 adhesion to biomaterials, leading the macrophage polarisation to their M2 reparative phenotype [16]. VTNC also interacts with the coagulation cascades, contributing to thrombus formation, and participates in the establishment of vascular homoeostasis, wound repair and tissue regeneration [35]. This protein promotes the osteogenesis by boosting the osteoblast differentiation [36]. APOE protein was also found predominantly on the SAE-Ti surfaces. This protein is involved in

the regulation of bone metabolism; its role in the bone tissue is probably related to its effect on vitamin K uptake into osteoblasts [37]. Proteins FA11, THRB and PROC play an important role in blood clotting. FA11 and THBR participate in the activation of the blood coagulation pathway. PROC is involved in the regulation of this pathway, through the inactivation of Va and VIIIa factors in the presence of phospholipids [38,39].

At the same time, proteomic analysis to the proteins more predominantly found in the silica sol-gel material (in comparison with the SAE-Ti) revealed a prevalence of proteins belonging to the complement system, namely CO5, CO8B, CO8A, CO7, C1R and CO6 [40], as well as the immunoglobulins IGJ, IGHM and IGHA1. This result was supported by the PANTHER analysis, which found a pronounced increase in the attachment of proteins related to immune system, from 2% on the uncoated SAE-Ti to 17% on the sol-gel coating (Figure 5). Interestingly, there was not found C-reactive protein adsorption, which, in a previous study, has been reported as related to acute/chronic inflammation processes and put forward as a bad biocompatibility biomarker [41].

This data unveils the relationship that an increment in immune response can suppose an increase on the activity of osteogenic markers (ALP and IL6) observed in the *in vitro* assays. This augmented immune system activation was also seen *in vivo* (Figure 4).

The implantation of biomedical devices entails a natural and significant immune response to the foreign material. The migration of white blood cells to the implantation site is caused by complement cascade proteins adsorbed on the surface of the implant. The consequent immune response is guided by cytokines that are activated and released by white blood cells, e.g., macrophages [42]. These cytokines can be responsible for producing a natural inflammatory reaction, giving the kick-start to the healing processes in the damaged tissue. An interaction between the host and the implant surface will result in the release of such molecules and trigger the activation of a series of cascades, determining the outcome of the implantation. The results obtained here show that an increase in the immune response to the implanted material might affect its bioactive

potential, as a result of the interactions between the immune and skeletal systems [43]. Such interactions, as long as the release of the immune product is controlled, might help to modulate the bioactivity of material towards the bone cells [44].

5. Conclusion

In summary, this study shows the importance of the adsorbed layer of proteins in the bioactivation of the material. The proteins from these layers, whose composition depends on the intrinsic characteristics of the material, might trigger the bioactivation process. Indeed, it has been found a significant deposition of complement-related proteins. These proteins intervene in processes such as the maintenance of cellular turnover, healing, proliferation and regeneration, apart from their role in the immune processes. This assumes a prolonged presence of the FBCGs on the regenerating tissue, and at the same time, a boost in the osteogenic potential, even though no effect on the *in vivo* regenerative potential is found.

Acknowledgements

This work was supported by the MAT 2014-51918-C2-2-R (MINECO), P11B2014-19, Universidad Jaume I under grant Predoc/2014/25, Generalitat Valenciana under grant Grisolia/2014/016 and Basque Government under grant Predoct/2016/1/0141. Authors would like to thank Antonio Coso and Jaime Franco (GMI-Ilerimplant) for their inestimable contribution to this study, and Raquel Oliver, Jose Ortega (UJI), Iraide Escobes (CIC bioGUNE), and Víctor Primo (IBV) for their valuable technical assistance.

References

[1] M. Özcan, C. Hämmerle, Titanium as a reconstruction and implant material in dentistry: Advantages and pitfalls, Materials (Basel)., 5 (2012) 1528–1545.

[2] X. Liu, P.K. Chu, C. Ding, Surface modification of titanium, titanium alloys, and related materials for biomedical applications, Mater. Sci. Eng. R Reports, 47 (2004) 49–121.

[3] A. Jemat, M.J. Ghazali, M. Razali, Y. Otsuka, Surface modifications and their effects on

titanium dental implants, Biomed Res. Int., 2015 (2015).

[4] S.L. Hirsh, D.R. McKenzie, N.J. Nosworthy, J.A. Denman, O.U. Sezerman, M.M.M. Bilek, The Vroman effect: Competitive protein exchange with dynamic multilayer protein aggregates, Colloids Surfaces B Biointerfaces, 103 (2013) 395–404.

[5] D.F. Williams, On the mechanisms of biocompatibility, Biomaterials, 29 (2008) 2941–2953.

[6] F. Romero-Gavilán, N.C. Gomes, J. Ródenas, A. Sánchez, F. , Mikel Azkargorta, Ibon Iloro, I.G.A. Elortza, M. Gurruchaga, I. Goñi, and J. Suay, Proteome analysis of human serum proteins adsorbed onto different titanium surfaces used in dental implants, Biofouling, 33 (2017) 98–111.

[7] S.N. Christo, K.R. Diener, A. Bachhuka, K. Vasilev, J.D. Hayball, Innate Immunity and Biomaterials at the Nexus: Friends or Foes, Biomed Res. Int., 2015 (2015).

[8] F. Romero-Gavilán, S. Barros-Silva, J. García-Cañadas, B. Palla, R. Izquierdo, M. Gurruchaga, I. Goñi, J. Suay, Control of the degradation of silica sol-gel hybrid coatings for metal implants prepared by the triple combination of alkoxysilanes, J. Non. Cryst. Solids, 453 (2016).

[9] M. Martínez-Ibáñez, M.J. Juan-Díaz, I. Lara-Saez, A. Coso, J. Franco, M. Gurruchaga, J. Suay Antón, I. Goñi, Biological characterization of a new silicon based coating developed for dental implants, J. Mater. Sci. Mater. Med., 27 (2016).

[10] M.J. Juan-Díaz, M. Martínez-Ibáñez, I. Lara-Sáez, S. da Silva, R. Izquierdo, M. Gurruchaga, I. Goñi, J. Suay, Development of hybrid sol–gel coatings for the improvement of metallic biomaterials performance, Prog. Org. Coatings, (2016).

[11] D. Arcos, M. Vallet-Regí, Sol-gel silica-based biomaterials and bone tissue regeneration, Acta Biomater., 6 (2010) 2874–88.

[12] E.M. Carlisle, Silicon: A possible factor in bone calcification, Science (80-.)., 167 (1970) 279–280.

[13] H. Mori, M. Manabe, Y. Kurachi, M. Nagumo, Osseointegration of dental implants in rabbit bone with low mineral density, J. Oral Maxillofac. Surg., 55 (1997) 351–361.

[14] C. Maniatopoulos, A. Rodriguez, D.A. Deporter, A.H. Melcher, An improved method for preparing histological sections of metallic implants, Int. J. Oral & Maxillofac. Implant., 1 (1986).

[15] J.R. Wisniewski, A. Zougman, N. Nagaraj, M. Mann, Universal sample preparation method for proteome analysis, 6 (2009) 3–8.

[16] Z. Chen, T. Klein, R.Z. Murray, R. Crawford, J. Chang, C. Wu, Y. Xiao, Osteoimmunomodulation for the development of advanced bone biomaterials, Mater. Today, 19 (2015) 304–321.

[17] A.E. Engberg, P.H. Nilsson, S. Huang, K. Fromell, O.A. Hamad, T.E. Mollnes, J.P. Rosengren-Holmberg, K. Sandholm, Y. Teramura, I.A. Nicholls, B. Nilsson, K.N. Ekdahl, Prediction of inflammatory responses induced by biomaterials in contact with human blood using protein fingerprint from plasma, Biomaterials, 36 (2015) 55–65.

[18] R. Latour, Biomaterials: protein-surface interactions, … Biomater. Biomed. Eng., (2005) 1–15.

[19] E.E. Golub, K. Boesze-Battaglia, The role of alkaline phosphatase in mineralization, Curr. Opin. Orthop., 18 (2007) 444–448.

[20] S. Ajai, A. Sabir, Evaluation of Serum Alkaline Phosphatase as a Biomarker of Healing Process Progression of Simple Diaphyseal Fractures in Adult Patients, Int. Res. J. Biol. Sci. Int. Res. J. Biol. Sci, 2 (2013) 2278–3202.

[21] Y. Li, C.-M. Bäckesjö, L.-A. Haldosén, U. Lindgren, IL-6 receptor expression and IL-6 effects change during osteoblast differentiation, Cytokine, 43 (2008) 165–173.

[22] P. Palmqvist, E. Persson, H.H. Conaway, U.H. Lerner, IL-6, Leukemia Inhibitory Factor, and Oncostatin M Stimulate Bone Resorption and Regulate the Expression of Receptor Activator of NF- B Ligand, Osteoprotegerin, and Receptor Activator of NF- B in Mouse Calvariae, J. Immunol., 169 (2002) 3353–3362.

[23] X.H. Liu, A. Kirschenbaum, S. Yao, A.C. Levine, Cross-talk between the interleukin-6 and prostaglandin E2 signaling systems results in enhancement of osteoclastogenesis through effects on the osteoprotegerin/receptor activator of nuclear factor-??B (RANK) ligand/RANK system, Endocrinology, 146 (2005) 1991–1998.

[24] R.L. Gallo, R.A. Dorschner, S. Takashima, M. Klagsbrun, E. Eriksson, M. Bernfield, Endothelial cell surface alkaline phosphatase activity is induced by IL-6 released during wound repair, J Invest Dermatol, 109 (1997) 597–603.

[25] F. Blanchard, L. Duplomb, M. Baud'huin, B. Brounais, The dual role of IL-6-type cytokines on bone remodeling and bone tumors, Cytokine Growth Factor Rev., 20 (2009) 19–28.

[26] K.M.R. Nuss, B. von Rechenberg, Biocompatibility issues with modern implants in bone - a review for clinical orthopedics, Open Orthop. J., 2 (2008) 66–78.

[27] S. Spriano, V. Sarath Chandra, A. Cochis, F. Uberti, L. Rimondini, E. Bertone, A. Vitale, C. Scolaro, M. Ferrari, F. Cirisano, G. Gautier di Confiengo, S. Ferraris, How do wettability, zeta potential and hydroxylation degree affect the biological response of biomaterials?, Mater. Sci. Eng. C, 74 (2017) 542–555.

[28] K. Rechendorff, M.B. Hovgaard, M. Foss, V.P. Zhdanov, F. Besenbacher, Enhancement of protein adsorption induced by surface roughness, Langmuir, 22 (2006) 10885–10888.

[29] D. Deligianni, N. Katsala, S. Ladas, D. Sotiropoulou, J. Amedee, Y. Missirlis, Effect of surface roughness of the titanium alloy Ti-6Al-4V on human bone marrow cell response and on protein adsorption, Biomaterials, 22 (2001) 1241–51.

[30] J. Vandercappellen, J. Van Damme, S. Struyf, The role of the CXC chemokines platelet factor-4 (CXCL4/PF-4) and its variant (CXCL4L1/PF-4var) in inflammation, angiogenesis and cancer, Cytokine Growth Factor Rev., 22 (2011) 1–18.

[31] N.H. Cho, S.Y. Seong, Apolipoproteins inhibit the innate immunity activated by necrotic cells or bacterial endotoxin, Immunology, 128 (2009) 479–486.

[32] Q. Li, Z. Zhai, W. Ma, Z. Qian, Anti-inflammatory effects of apoprotein AI are mediated via modulating macrophage polarity, Chinese J. Cardiol., 42 (2014).

[33] D. Baitsch, H.H. Bock, T. Engel, R. Telgmann, C. Müller-Tidow, G. Varga, M. Bot, J. Herz, H. Robenek, A. Von Eckardstein, J.-R. Nofer, Apolipoprotein e induces antiinflammatory phenotype in macrophages, Arterioscler. Thromb. Vasc. Biol., 31 (2011).

[34] T.E. Mollnes, M. Kirschfink, Strategies of therapeutic complement inhibition, Mol.

Immunol., 43 (2006) 107–121.

[35] D.I. Leavesley, A.S. Kashyap, T. Croll, M. Sivaramakrishnan, A. Shokoohmand, B.G. Hollier, Z. Upton, Vitronectin - Master controller or micromanager?, IUBMB Life, 65 (2013) 807–818.

[36] R.M. Salasznyk, W.A. Williams, A. Boskey, A. Batorsky, G.E. Plopper, Adhesion to Vitronectin and Collagen I Promotes Osteogenic Differentiation of Human Mesenchymal Stem Cells, J. Biomed. Biotechnol., 2004 (2004) 24–34.

[37] A. Niemeier, T. Schinke, J. Heeren, M. Amling, The role of Apolipoprotein E in bone metabolism, Bone, 50 (2012) 518–524.

[38] P.N. Walsh, Roles of platelets and factor XI in the initiation of blood coagulation by thrombin, Thromb. Haemost., 86 (2001).

[39] D. Josic, L. Hoffer, A. Buchacher, Preparation of vitamin K-dependent proteins, such as clotting factors II, VII, IX and X and clotting inhibitor Protein C, J. Chromatogr. B Anal. Technol. Biomed. Life Sci., 790 (2003) 183–197.

[40] K. Murphy, P. Travers, M. Walport, The complement system and innate immunity, Janeway's Immunobiol., 7 (2008) 61–81.

[41] N. Araújo-Gomes, F. Romero-Gavilán, A.M. Sanchez-Pérez, M. Gurruchaga, M. Azkargorta, F. Elortza, M. Martínez-Ibáñez, I. Iloro, J. Suay, I. Goñi, Characterization of serum proteins attached to distinct sol – gel hybrid surfaces, (2017) 1–9.

[42] G.S.A. Boersema, N. Grotenhuis, Y. Bayon, J.F. Lange, Y.M. Bastiaansen-Jenniskens, The Effect of Biomaterials Used for Tissue Regeneration Purposes on Polarization of Macrophages, Biores. Open Access, 5 (2016) 6–14.

[43] F. Romero-Gavilán, A.M. Sanchez-Pérez, N. Araújo-Gomes, M. Azkargorta, I. Iloro, F. Elortza, M. Gurruchaga, I. Goñi, J. Suay, Proteomic analysis of silica hybrid sol-gel coatings: a potential tool for predicting the biocompatibility of implants in vivo, Biofouling, In press (2017).

[44] J. Lorenzo, M. Horowitz, Y. Choi, Osteoimmunology: Interactions of the bone and immune system, Endocr. Rev., 29 (2008) 403–440.